Pergamon

Journal of Atmospheric and Solar-Terrestrial Physics, Vol. 60, No. 1, pp. 115–120, 1998

1364–6826/98 $19.00+0.00

PII: S1364–6826(97)00051–5

Determining the velocity of the interference pattern by analyzing three mutually orthogonal projections of the radio signal field vector. Part I. numerical simulation

E. L. Afraimovich* and K. S. Palamartchouk

Institute of Solar-Terrestrial Physics, Siberian Division of Russian Academy of Science (ISTP SD RAS), 664033 Irkutsk, P.O. Box 4026, Russia

(*Received* 31 *October* 1996; *in revised form* 20 *June* 1997; *accepted* 4 *July* 1997)

Abstract—This article suggests using a spectral polarization method for measuring the velocity of displacement of the interference pattern by analyzing three mutually orthogonal projections of the radio signal field vector using a single receiving antenna. The initial stage of analysis involves calculating complex Doppler spectra of time variations of these projections. Thereupon, for each spectrum component, these data are used to determine angle of arrival spectra. In conjunction with data on Doppler frequency shifts, this procedure makes it possible to estimate the velocity and direction of interference pattern displacement. We give the equations to illustrate the proposed technology and simulation results, showing that it is essentially possible to realize this idea. © 1998 Published by Elsevier Science Ltd

INTRODUCTION

The preponderance of data on ionospheric dynamics was obtained from ground-level measurements of spatio-temporal characteristics of the interference pattern (phase and amplitude) of the ionospherically reflected radio signal at vertical or slightly-oblique incidence in the LF, MF and HF ranges, or at the transionospheric propagation from discrete radio sources or satellite-borne transmitters in the VHF range. The problem of the match between interference pattern parameters and corresponding electron density irregularities at a certain height in the ionosphere are typically solved in terms of a suitable 'phase screen' model, and we shall not take it up here.

Such measurements were always made with spatially separated receiving antennas, beginning with the simplest version of three antennas in the pioneering article by Mitra (1949) and ending with large multi-antenna amplitude matrices (Brownlie *et al.*, 1973) or phased antenna arrays and radio astronomical interferometers (Jacobson *et al.*, 1991, 1995).

The disadvantage of the conventional method was the persistent need to ensure the required spatial aperture, which limited the possibility of determining characteristics of the motion when a large spatial separation between the antennas was to be used. Moreover, this led to a serious limitation on the possibility of studying space-time characteristics of the reflecting surface in the case of remote soundings from moving platforms (aircraft and satellites).

The proposed technique can also improve the spatial resolution when carrying out remote sounding operations from moving platforms. This idea seems to have been pioneered in a monograph (Afraimovich, 1982) but has not yet received an appropriate development. Of course, we are by no means of the opinion that the proposed technique is capable to supplant the conventional method; in cotrast, it may be useful as a substantial adjunct to it. The objective of this article is to demonstrate that it is in principle possible to measure interference pattern velocity characteristics of the radio signal at the terrestrial surface level without recourse to a conventional spaced-antenna method. A description of the hardware and software system, and also data of an experimental testing of the method in comparison with angle-of-arrival measurements using a standard HF direction-finder, are currently being generalized and will be reported elsewhere.

DETERMINING THE INTERFERENCE PATTERN VELOCITY FOR SPACED-ANTENNA RECEPTION

We start by considering a reasonably general example of vertical-incidence soundings, and the main prin-

*E-mail: afra@iszf.irk.ru

ciples of interference pattern velocity determination in terms of a simple interference model (Afraimovich, 1982). The major implications of this model are consistent with numerous existing methods of data analysis for coherent spaced antenna reception (see, for example, Pfister (1971); Afraimovich *et al.* (1978); Jacobson and Carlos (1989)).

A complex amplitude of the radio signal at a given point of the terrestrial surface with the coordinates $x = y = 0$ at the time t may be represented as a discrete set of s-modes (rays);

$$\tilde{A}(x,y,t) = \sum_{s=1}^{n} r_s \exp(j(kP_s + \varphi_s(0))) \quad (1)$$

where r_s is the amplitude, P_s is the signal phase path, $k = 2\pi/\lambda$; λ is the wavelength, $\varphi_s(0)$ is the initial phase, and n is the number of modes. Consider the spatial properties of A in the approximation of closely spaced antenna reception. In this case it is assumed that the distance between the receiving antennas d_x and d_y are much smaller than the typical spatial scale of a disturbance in the antenna array plane, and that the time interval Δt between the counts is much smaller than the disturbance time scale, so that the influence of second derivatives may be neglected.

In this case the phase front of the signal s-component may be considered to be plane and the coefficient r_s to be independent of the coordinate x (directed northward) and y (directed westward), so that the signal on the spaced antennas differs only by the phase delay dependent on the antenna location and the time t.

$$\begin{aligned} kP_s(x,y,t) &= k_{x,s}x + k_{y,s}y - \omega_s t \\ k_{x,s} &= k \sin\theta_s \cos\psi_s \\ k_{y,s} &= k \sin\theta_s \sin\psi_s \end{aligned} \quad (2)$$

where θ is the elevation reckoned from the zenith, ψ is the azimuthal angle of arrival measured from the northward direction in the westward direction (see Fig. 1), and ω is the frequency Doppler shift.

The velocity V_s and the direction ψ_s of the phase front of the radio signal s-component are then determined by values of the angles of arrival and of the Doppler frequency;

$$V(\omega_s) = \omega_s / 2\sqrt{k_{x,s}^2 + k_{y,s}^2} \quad (3)$$

$$\psi(\omega_s) = \arctan(k_{y,s}/k_{x,s})$$

Corresponding, widely-known methods of spectral analysis of the complex amplitude are in use to resolve individual spectrum components and to determine velocity parameters using (3) (see, for example, Pfister (1971); Afraimovich *et al.* (1978); Jacobson and Carlos (1989)). Amplitude variations of the reflected multimode signal are formed by interference of all components in (1); a detailed analysis is performed by Afraimovich (1982) and other authors;

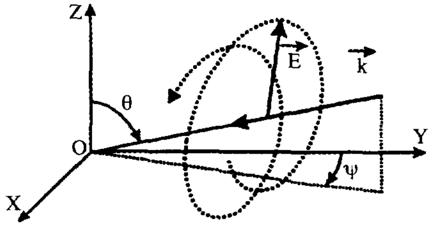

Fig. 1. Experimental geometry. The direction of incidence of the radio wave with the wave number $\vec{k}$ is specified by the angle of elevation θ measured from the z-axis, and by the azimuth ψ measured from the y-axis toward the x-axis. The field vector $\vec{E}$ describes a spiral whose form is determined by the wave polarization parameters.

$$|\tilde{A}|^2 = \sum_q \sum_s r_q r_s \cos(k\Delta_{q,s}P_s + \Delta_{q,s}\varphi(0))$$

$$\begin{aligned} k\Delta_{q,s}P(x,y,t) &= \Delta_{q,s}k_x x + \Delta_{q,s}k_y y - \Delta_{q,s}\omega t \\ \Delta_{q,s}k_x &= \sin\theta_q \cos\psi_q - \sin\theta_s \cos\psi_s \\ \Delta_{q,s}k_y &= \sin\theta_q \sin\psi_q - \sin\theta_s \sin\psi_s \\ \Delta_{q,s}\omega &= \omega_q - \omega_s \end{aligned} \quad (4)$$

The velocity $V_{q,s}$ and direction $\psi_{q,s}$ of the partial amplitude front displacement is determined by differences of the angles of arrival and Doppler frequencies of the (q,s)-components of signal;

$$V_{q,s} = \frac{\Delta_{q,s}\omega}{2\sqrt{(\Delta_{q,s}k_x)^2 + (\Delta_{q,s}k_y)^2}}$$

$$\psi_{q,s} = \arctan(\Delta_{q,s}k_y/\Delta_{q,s}k_x) \quad (5)$$

Thus, a most general version of determining the interference pattern velocity for coherent reception is based, in one way or another, upon separating the spectrum components of the complex signal, with a subsequent determination of Doppler frequencies and angles of arrival of the spectrum components;

$$\begin{aligned} \omega_s &= \Delta\varphi_{q,s}/\Delta t \\ k_{x,s} &= \Delta\varphi_{x,s}/d_x \\ k_{y,s} &= \Delta\varphi_{y,s}/d_y \end{aligned} \quad (6)$$

where $\Delta\varphi_t$, $\Delta\varphi_x$, $\Delta\varphi_y$, are the phase differences, and d_x, d_y are the bases of spacing in the corresponding variables when the receiving antennas are located at the corners of a right angle triangle. Actually there exists a plethora of methods for determining the interference pattern velocity and direction, not necessarily involving a preliminary calculation of Doppler frequencies and angles of arrival of the signal; all of them, however, may be brought to a form that is adopted in this article.

DETERMINING THE INTERFERENCE PATTERN VELOCITY WITHOUT RECOURSE TO SPATIAL SEPARATION

Morgan and Evans (1951) showed that in free space the complex amplitudes of three mutually orthogonal projections of a single mode regular signal field determine parameters of the ellipse of polarization and the direction of rotation of the polarization vector, as well as the angles of arrival ψ and θ (the orientation of the wavefront). The previous-listed parameters constitute a description of a full field vector of a plane radio wave and are related to complex amplitudes of the field projections by a system of transcedental equations (the z-axis pointing to the zenith).

$$\tilde{A}_x = A_x \exp(j\varphi_x)$$
$$\tilde{A}_y = A_y \exp(j\varphi_y)$$
$$\tilde{A}_z = A_z \exp(j\varphi_z) \quad (7)$$

Without going into a description of the algorithms caused by Morgan and Evans (1951), we shall give only formulas defining the angles of arrival of a plane wave in free space;

$$\tan\psi = A_x \sin(\varphi_x - \varphi_z)/A_y \sin(\varphi_z - \varphi_y)$$
$$\tan^2\theta = \frac{A_x^2 A_z^2 \sin^2(\varphi_x - \varphi_z) + A_z^2 A_y^2 \sin^2(\varphi_z - \varphi_y)}{A_x^2 A_y^2 \sin^2(\varphi_y - \varphi_x)} \quad (8)$$

The principle of angle of arrival determination from the measurements, made at a single point, of three projections of the electric or magnetic fields of the wave is well known and is used in VLF radiation research; Calvert *et al.* (1995) suggest that such technology should be used for magnetospheric soundings.

Of course, it is highly tempting to exploit the possibility of determining parameters of a full field vector, especially the angles of arrival and the interference pattern velocity, using a single antenna. However, formulae (8) can be used directly in a data treatment only for a strictly regular single mode signal. External noise and signal scattering contribute to an increase of the error of measurement, and the multimode approach with similar values of mode amplitudes causes irreversible interference distortions, which imposes a drastic limitation on the use of this method in research and applied radio engineering. The resolution of this issue involves mode separation; research systems typically use pulsed ionospheric soundings, which on some occasions lead to successful mode separation. However, such a procedure is unsuitable for the continuous or modulated radio signal of broadcasting stations in the LF, MF, and HF ranges.

This problem is resolved in large part by a method for analyzing a full field vector of the radio wave based on complex Doppler filtering of modes as suggested by Afraimovich *et al.* (1979). This method, in essence, implies that all algorithms for calculating parameters of a full field vector using a system of equations with respect to mutually orthogonal projections utilize, instead of the complex amplitudes of projections, complex amplitudes of the components of a complex Doppler spectrum of these projections, i.e. the amplitude $S_x(\omega)$, $S_y(\omega)$, $S_z(\omega)$, and phase $\Phi_x(\omega)$, $\Phi_y(\omega)$, $\Phi_z(\omega)$, spectra, where ω is the angular frequency. These spectra are calculated for x, y, z—the complex amplitudes of the signal from the output of corresponding mutually orthogonal antennas using Fast Fourier Transform (FFT) algorithms and appropriate time or spectral windows.

Thus, in equation (8), we suggest that the complex amplitudes of the components of a complex Doppler spectrum of three projections of the field, rather than individual measured values of A_x, A_y, and A_z, should be considered. In much the same way, the angle of arrival spectrum is calculated; for conditions of free space, these spectra take the form;

$$\tan\psi(\omega) = S_x(\omega)\sin(\Delta_{xz}(\omega))/S_y(\omega)\sin(\Delta_{zy}(\omega))$$
$$\tan^2\theta(\omega) = \frac{S_x^2(\omega)S_z^2(\omega)\sin^2(\Delta_{zx}(\omega)) + S_z^2(\omega)S_y^2(\omega)\sin^2(\Delta_{zy}(\omega))}{S_x^2(\omega)S_y^2(\omega)\sin^2(\Delta_{yx}(\omega))} \quad (9)$$

where $\Delta_{yx}(\omega) = \varphi_y(\omega) - \varphi_x(\omega)$, $\Delta_{zy}(\omega) = \varphi_z(\omega) - \varphi_y(\omega)$, $\Delta_{xz}(\omega) = \varphi_x(\omega) - \varphi_z(\omega)$, respectively.

Complex Doppler filtering makes it possible not only to separate interfering modes but also to ensure a high noise immunity of measurements and, as a consequence, a high stability of the solution of the transcedental equations. Algorithms of the method should be used only upon checking Doppler filters for residual interference (Afraimovich, 1982). Obtaining an angle of arrival spectrum is of significance in its own right; in terms of our proposed method, resulting values of $\psi(\omega)$ and $\theta(\omega)$ are used to reconstruct the spatial characteristics of the interference pattern by invoking equation (2) with the purpose of obtaining the spectra $k_x(\omega)$ and $k_y(\omega)$.

Several avenues for analysis may then be chosen. A most general procedure involves reconstructing the space-time pattern of $\tilde{A}(x,y,t)$ by synthesizing the interference pattern using equation (1) and equation (4). The interference pattern reconstructed in such a way can then be handled using any one of the existing methods of analysis, also with the objective of reconstructing the form of the space-time correlation function.

Thus, the solution of the problem formulated is governed by the accuracy with which the radio wave angles of arrival can be determined by using a three component antenna.

NOISE AND INTERFERENCE EFFECTS ON THE RECONSTRUCTION OF ANGLES OF ARRIVAL (SIMULATION)

Obviously there exists a host of factors which can hinder the feasibility of this method. Primarily they include noise and intermodal interference. In an attempt to investigate the influence of these factors, we analyzed the potentialities of the method through the use of a computer simulation. Possible systematic errors in determining angles of arrival, caused by the mutual influence of the antennas and the surrounding medium, are not treated in this article.

The first stage of simulation involved obtaining series of instantaneous counts of projections (7) of the electromagnetic wave $\vec{E}$ -field vector onto three mutually perpendicular antennas (see Fig. 1). This was done by calculating the scalar product of the $\vec{E}$ -field vector with unit vectors along the axes OX, OY and OZ, or, in more general cases, by arbitrary unit vectors. The $\vec{E}$ -field vector was calculated for each instant of time based on the specified (for each particular run) amplitude and angle of arrival of the radio wave, and on the ratio of the semi-axes of the polarization ellipse and their orientation in space. The results reported below were all obtained for a circularly polarized signal with a clockwise sense. A generator of pseudorandom numbers was also used to simulate the noise whose amplitude also changed.

In the second stage, the resulting series were subjected to a direct Fourier transform. After that, angles of arrival were calculated by formula (9) for each of the spectral components of amplitude $S(\omega)$ and difference-phase $\Delta(\omega)$ spectra. Figure 2 presents examples of simulated amplitude $S(f)$ and phase-difference $\Delta(f)$ spectra of the two-mode signal simulated for one of projections.

The results presented below were all obtained for the components whose amplitude was above the specified threshold $\epsilon = 0.1$. All model calculations were

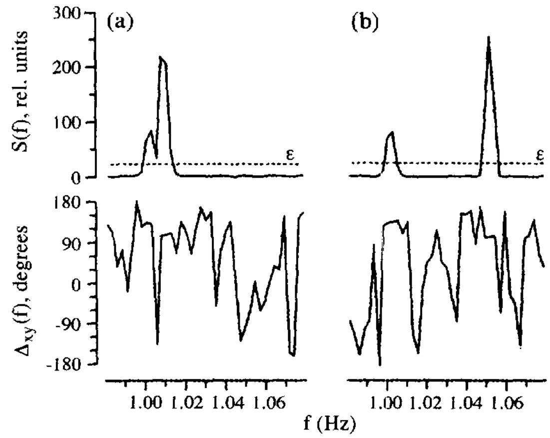

Fig. 2. Examples of simulated amplitude $S(f)$ (top) and phase-difference $\Delta(f)$ (bottom) spectra of the two-mode signal simulated for one of projections. A series of 2048 points, with the signal frequency $f = \omega/2\pi = 1$ Hz and the count frequency 10 Hz, was used. Mode separation in frequency $\Delta f = \Delta\omega/2\pi$. Dashed lines show the thresholds ϵ which in this case constitute 0.1 of the maximum harmonic amplitude, below which it is assumed that $S(f) = 0$. (a, $\Delta f = 0.007$ Hz; b, $\Delta f = 0.05$ Hz).

performed with series $1024 = 2^{10}$, $2048 = 2^{11}$ and $4096 = 2^{12}$ points long for the sake of convenience when applying a Fast Fourier Transform. The difference in lengths of the series is responsible for a difference in the spectral line width. In actual practice, it is appropriate to reduce the line width to a minimum, which would require increasing the data accumulation time; yet it should not exceed the typical non-stationarity period which is about 300 s for the HF range.

Figure 3 presents results derived by analyzing the reconstruction accuracy of angles of arrival on the basis of the above transforms for different values of the signal/noise ratio. Research results are shown in one octant only. Formulas (9) define uniquely the angle ψ, and the angle θ is defined only in the range 0°–90°, with its sign left indefinite. The solutions of equation (9), lying in different octants, have the same behaviour. In practice, for measuring angles of arrival and for reconstructing the form of the interference pattern, it is always sufficient to determine θ but not its sign.

Calculations were carried out with a series with 4096 points in each, with the useful signal frequency of 1 Hz, under the assumption that the count frequency is 10 Hz. The root-mean-square angular diameter of a circle on a sphere $\Delta\alpha$ (θ,ψ), to which the calculated points correspond, was used as the parameter to esti-

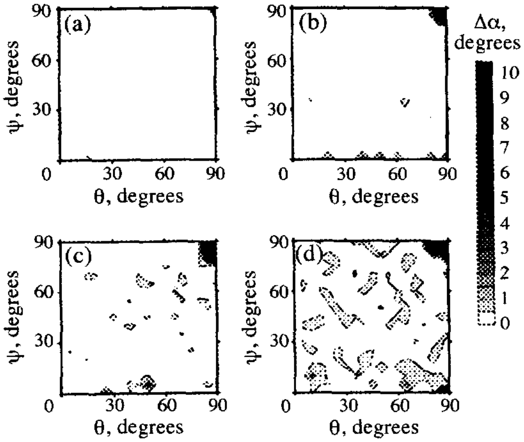

Fig. 3. Results derived by analyzing the accuracy of angle of arrival determination depending on the Signal/Noise (S/N) ratio. The value of $\Delta\alpha(\theta,\psi)$ is shown by different shadings in accordance with the half-tone scale at the side. (a, S/N = 2.0; b, S/N = 1.0; c, S/N = 0.66; d, S/N = 0.5).

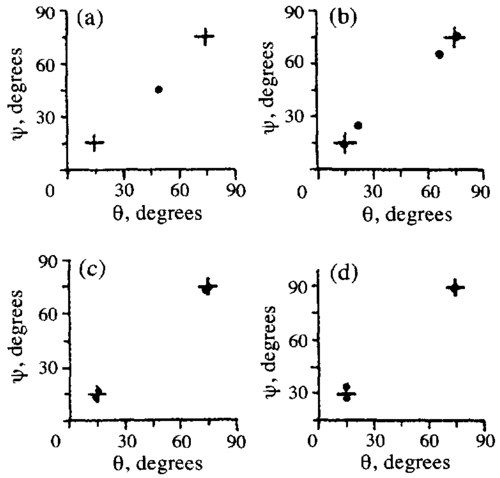

Fig. 4. Results derived by analyzing the accuracy of angle of arrival determination in the presence of two modes of identical amplitude and the frequency difference Δf. Crosses show the specified directions ($\theta = 15°$, $\psi = 15°$) and ($\theta = 75°$, $\psi = 75°$); heavy dots show the reconstructed directions). (a, $\Delta f = 0.0$ Hz; b, $\Delta f = 0.02$ Hz; c, $\Delta f = 0.03$ Hz; d, $\Delta f = 0.05$ Hz.).

mate the accuracy. The centre of the circle lies at the point whose angular coordinates θ and ψ were specified as the origin.

If the noise amplitude is zero, the angles are reconstructed within the accuracy of the computer computations. When the noise level increases, unreliable regions of the octant are beginning to emerge as θ and ψ approach 90°, and further also when ψ tends to 0°. In this case the diameter of the spot of spread $\Delta\alpha$ (θ,ψ) reaches 10°. In most of the octant, however, when S/N is no worse than 1.0, $\Delta\alpha$ (θ,ψ) does not exceed 0.5°.

Figure 4 presents the results of analysis of the reconstruction accuracy of angles of arrival on the basis of the above transforms for the case of the interference of two modes, with specified values of Doppler frequency and angles of arrival, and the ratio S/N = 5.0. Series with 1024 points were used, with 1 Hz signal frequency and with 10 Hz count frequency. Under such conditions, the spectral line width is 0.021 Hz.

In the absence of frequency separation, both modes merge into one, and the reconstructed direction (Fig. 4(a)) lies midway between the two specified directions. With a separation by $\Delta f = 0.01$ Hz, the interference effect is very large-phase and amplitude relationships undergo such changes that the reconstructed angles of arrival do not lie within the octant under consideration (this case is not shown in Fig. 4). However, such a small frequency spread with a large angular spread (tens of degrees) is actually rare. But with a frequency separation of the modes comparable with the spectral line width, the modes are resolved quite confidently (Fig. 4(b)). With a further increase in frequency spread (Fig. 4(c) and 4(d)), the quality of mode separation is improved.

CONCLUSIONS

The results suggest the following conclusions:

1. the accuracy of angle-of-arrival determination using the proposed method depends on values of θ and ψ specified (in most of the angular range these are about 1°-with the signal/noise ratio no worse than 1.0);
2. there exist sectors of angles, in which the method does not warrant a reasonable accuracy; however, they are not large (a few degrees), and in practice the receiving antenna can always be oriented so that such a situation is avoided, because the width of the angular spectrum does not usually exceed 10°;
3. Doppler separation makes it possible to determine arrival directions of modes separated in frequency by about the natural spectral line width, to an accuracy better than 10°; with an increase in the frequency spread to a value larger than the line width by a factor of 2–3, the interference ceases to play a marked role.

Acknowledgements—The authors thanks V.G. Mikhalkovsky for his assistance in preparing the English version of the manuscript. This work was supported by the Russian Foundation for Fundamental Research under Grants 96-05-64162 and 97-02-96060.

REFERENCES

Afraimovich, E. L., Vugmeister, B. O., Zacharov, V. N., Kalikhman, A. D. and Korolev, V. A. (1978) Experimental investigation of fluctuations of radio signal Doppler frequencies and angles of arrival by vertical-incidence sounding of the ionospheric F2 layer. *Izvestia Vuzov Radio Physics* **21,** 338–347.

Afraimovich, E. L., Agafonnikov, Yu. M. and Polimatidi, V. P. (1979) USSR Inventor's Certificate No. 650026. *Official Bulletin of USSR Patent Department, No.* **8,** 153.

Afraimovich, E. L. (1982) *Interference Methods of Ionospheric Radio Sounding*, Nauka, Moscow.

Brownlie, G. D., Dryburgh, L. G. and Whitehead, J. D. (1973) Pencil beam radar for ionospheric research. *Nature, Phys. Sci.* **243(129),** 112.

Calvert, W., Benson, R. F., Carpenter, D. L., Fung, S. F., Gallagher, D. L., Green, J. L., Haines, D. M., Reiff, P. H., Reinisch, B. W., Smith, M. F. and Taylor, W. W. L. (1995) The feasibility of radio sounding in the magnetosphere. *Radio Science* **30(5),** 1577–1595.

Jacobson, A. R. and Carlos, R. C. (1989) Coherent-array HF doppler sounding of travelling ionospheric disturbances. 1. Basic. technique. *Journal of Atmospheric Physics* **51,** 257–309.

Jacobson, A. R., Massey, R. S. and Erickson, W. C. (1991) A study of transionospheric refraction of the radio waves using the Clark Lake Radio Observatory. *Annal. Geophys.* **9,** 546–552.

Jacobson, A. R., Carlos, R. C., Massey, R. S. and Wu, G. (1995) Observations of travelling ionospheric disturbances with a satellite-beacon radio interferometer: Seasonal and local-time behavior. *Journal of Geophysical Research* **100,** 1653–1665.

Mitra, S. N. (1949) A radiomethod of measuring winds in the ionosphere. *Proc. IEE* **96,** 441–482.

Morgan, M. and Evans, W. (1951) Synthesis and analysis of elliptic polarization loci in terms of space-quad quadrature sinusoidal components. *Proc. IRE* **39,** 552–556.

Pfister, W. (1971) The wave-like nature of inhomogeneities in the E-region. *Journal of Atmospheric and Terrestrial Physics* **33,** 999–1025.